NASA CONTRACTOR REPORT 165858

NASA-CR-165858
19820018362

FLOWS OVER WINGS WITH LEADING-EDGE VORTEX SEPARATION

B.M. RAO AND B. MASKEW

ANALYTICAL METHODS, INC.
Redmond, Washington 98052

Contract NAS1-16155
APRIL 1982

NASA
National Aeronautics and
Space Administration

Langley Research Center
Hampton, Virginia 23665

TABLE OF CONTENTS

LIST OF FIGURES

SUMMARY

The unsteady cross-flow analogy allows us to reduce the steady three-dimensional separation flow problem into an unsteady two-dimensional flow problem in which the section shape changes with time. The two-dimensional VORSEP code is extended to the case of arbitrary body growth rates in order to generate the initial vortex structures for the NASA-Langley/Boeing three-dimensional Free-Vortex-Sheet (FVS) code.

Automatic procedures to reduce the wing geometry definintion to a set of cross-flow plane sections corresponding to the locations of the time-step solutions and to generate the effective source distribution on each cross-flow section to represent the section normal growth across the following steps are incorporated in the VORSEP code. Also, the wake shedding model is improved by adopting a redistribution scheme which improves the stability of the free sheet development with time. The improved wake shedding model combined with the redistribution scheme alleviated the numerical instabilities associated with the vortex roll-up.

The modified VORSEP is applied to several test cases: a thin delta wing, an ogee wing, and a bent plate. The preliminary results look very promising.

1.0 INTRODUCTION

1.1 Background

Flow separations are certain to occur on thin, highly swept wings at moderate to high angles of attack. The flow separations usually take the form of two free vortex layers joined to the leading edges of the wing which roll up to form spiral-shaped vortex sheets above the surface. These vortex separations lead to important nonlinear lift characteristics. A recent review (1) of the subject describes a number of inviscid fluid models which have been used in the past to predict the vortex characteristics.

The suction analogy put forward by Polhamus (2) predicts the wing lift for a broad class of wing planforms, but does not provide flow-field details or surface pressure-distribution information. Various methods based on conical flow assumptions (3), (4) and (5), provide such details for a limited class of slender configurations, but fail towards the trailing-edge region because the trailing-edge Kutta condition is excluded.

More recently, an improved panel method (Boeing FVS, (6)) has been applied to the problem. The approach is necessarily based on an iterative procedure in order to satisfy all the boundary conditions on the solid surface, the free vortex sheet, feeding sheet and vortex core. Although the calculations start with an initial vortex structure based on conical flow assumptions, the number of iterations required for convergence may be quite large. This poses a severe problem for the case of thick sections and other situations (e.g., general planforms) where the initial conical flow assumptions are not valid.

Under an earlier contract from NASA Langley Research Center (NAS1-15495), Analytical Methods, Inc. developed an analysis (7) and a pilot code (VORSEP, (8)) for the calculation of vortex/surface interference, adopting a singularity panel method. The analysis and the code include the development of a computational procedure for vortex separation from a sharp-edged plate as well as from a growing thick body using a time-stepping approach.

1.2 Present Approach

The main objective of the present work is to extend the present two-dimensional VORSEP code for vortex separation to the case of arbitrary body growth rates in order to generate the initial vortex structures for the Boeing three-dimensional (FVS) code. A brief technical discussion and theoretical background are presented in Sections 3.0 and 4.0, respectively. In Section 5.0, the body growth and free-sheet shedding models are described. Procedures to reduce the wing geometry definition to a set of cross-flow plane sections corresponding to the locations of the time-step solutions and to generate the effective source distribution on each cross-flow section to represent the section normal growth across the following

step are developed. The free-sheet shedding model is improved by adopting a redistribution scheme which improved the stability of the free sheet development with time. In Section 6.0, the results for three test cases, a delta wing, ogee wing and a rectangular bent plate are presented.

2.0 NOMENCLATURE

Except where dimensions are given, the variables listed below are regarded as dimensionless.

A,B	Influence coefficient
F	Defined in Section 4.0
$\underline{G}$	Growth vector
M	Number of wake panels
N	Number of surface panels
$\underline{r}$	Radius vector
γ	Vorticity strength
Δt	Time-step increment
θ_{merge}	Angle beyond which vortices on the free sheet are merged with the vortex core in the vortex roll-up calculations
μ	Doublet strength
σ	Source strength
ϕ	Perturbation potential
ϕ_∞	Onset flow potential

3.0 TECHNICAL DISCUSSION

The initial vortex structure input to the three-dimensional code (BOEING FVS) is currently based on self-similar solutions in cross-flow planes proceeding chordwise across the swept wing. With general wing planforms, and particularly with thick sections and leading-edge camber, self-similarity no longer applies and the conditions for conical flow are lost. However, in priciple, an initial vortex structure can still be generated by using the unsteady cross-flow analogy. With this assumption, the steady three-dimensional flow problem is transformed into an unsteady two-dimensional flow problem in which the section shape changes with time, Figure 1. An example of such an application is given in (9) for the separated flow over a body of revolution.

Most of the previous applications of the unsteady cross-flow analogy have used a transformation based on the flow about a circle. In the present investigation, a time-stepping procedure is applied for the computation of the development of the vortex core in the cross-flow plane using the two-dimensional panel method (VORSEP).

The VORSEP code has demonstrated the feasibility of such an approach in a simple situation of uniform growth rate of an elliptical section, Figure 2 (from (7)). In the present investigation, the code is extended to the more general case by allowing arbitrary sections at each time step. The growth rate of each part of the section is then computed on a panel by panel basis rather than being a uniform overall growth factor. The details of the input and computational procedures for the time-dependent arbitrary sections are presented in Section 5.0. Also, the shedding model and the free vortex sheet calculation procedure are improved by adopting a redistributed vorticity with equal length panels along the free sheet. The details of this refinement are also presented in Section 5.0.

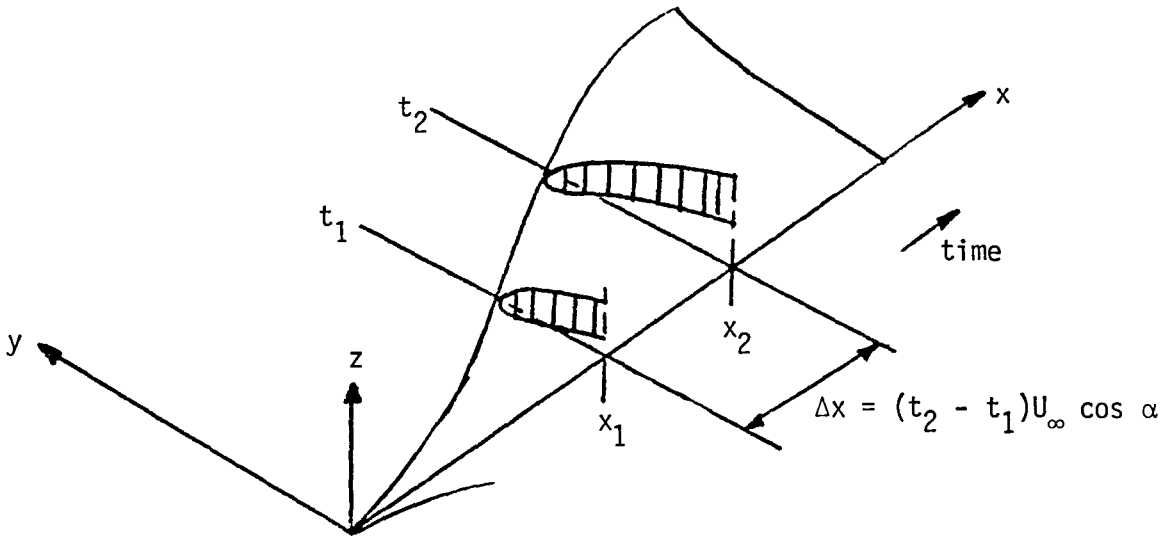

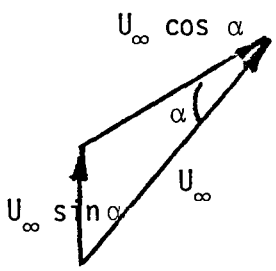

F(x) Factor from Suction Analogy Loading to Simulate Trailing Edge Kutta Condition

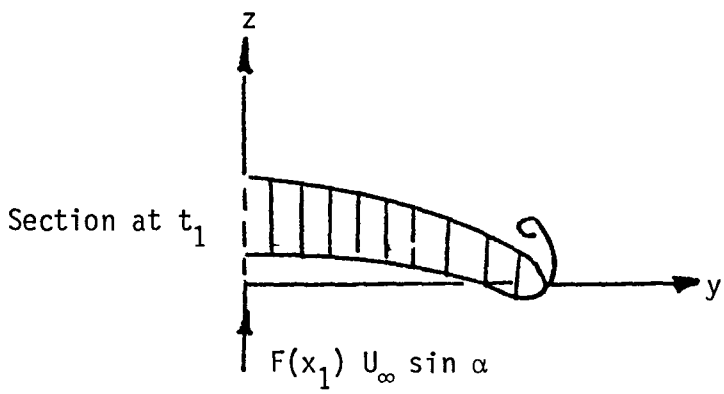

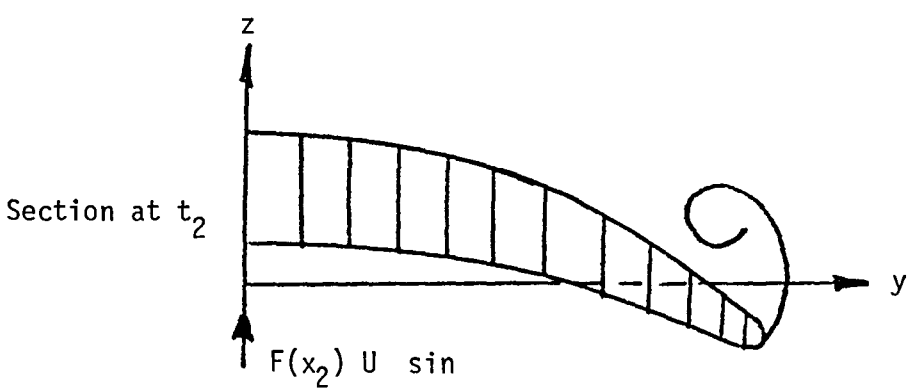

Figure 1. Unsteady Cross-Flow Analogy.

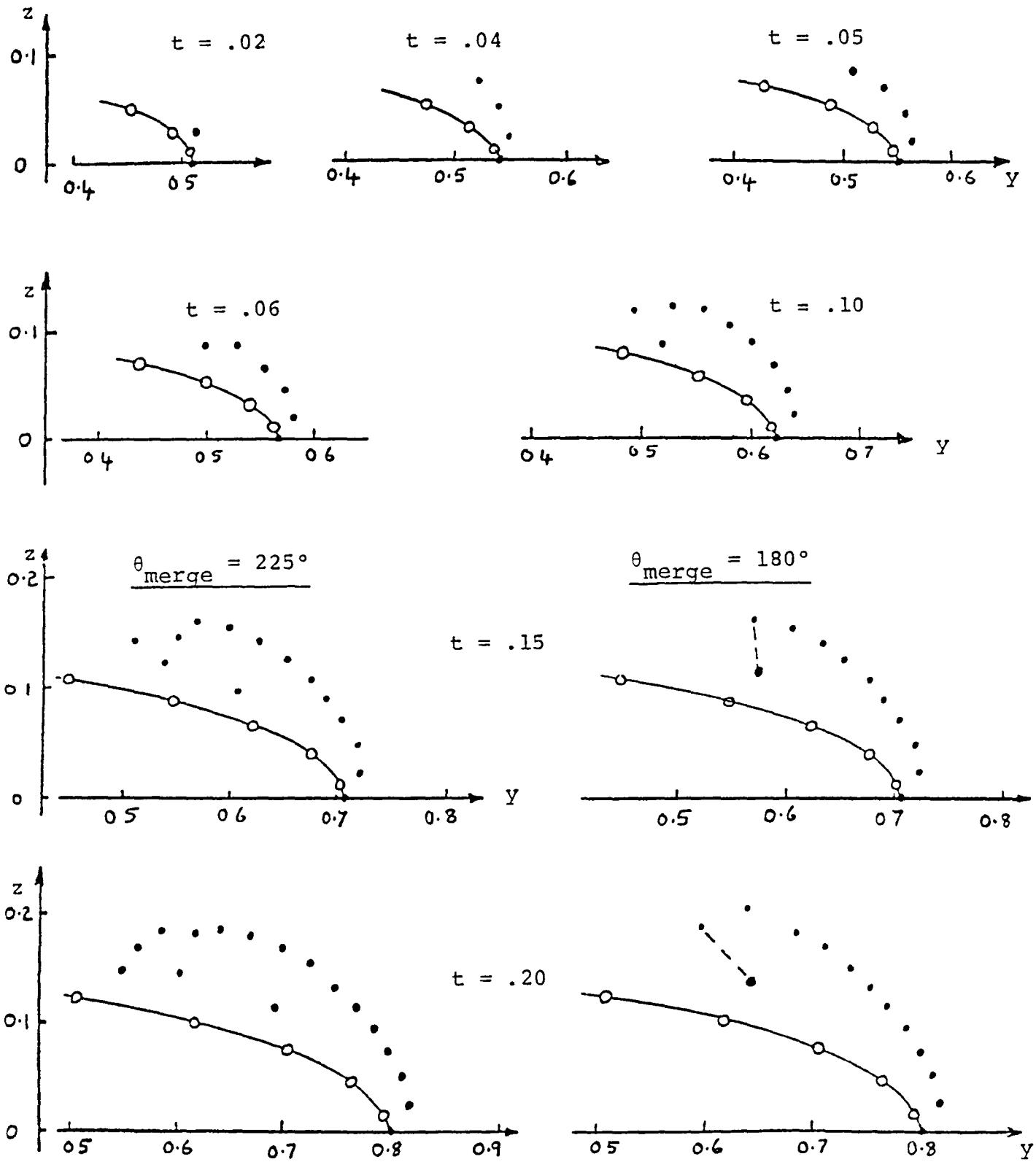

Figure 2. History of the Vortex Structure on the Growing 5:1 Ellipse. Growth Factor = 1.025 at Each Time Step. Time Interval = .01.

4.0 THEORY

A complete description of the panel method is presented in (7). A brief outline of the panel method boundary condition equation is presented here as it pertains to the body "growth" rate.

The panel method in the VORSEP code is based on doublet and source singularities distributed on flat panels representing the section surface. The doublet distribution is continued onto the free sheet. At each time step the boundary condition of zero total velocity potential is applied on the inside of the section at a control point (mid) on each panel. With this formulation the total tangential velocity on the exterior (wetted) surface is the doublet gradient and the source value there is proportional to ($\frac{1}{2}\pi$) the total normal velocity. Clearly, in the steady case the source distribution is zero (unless boundary displacement effects are being represented by the transpiration technique). In the present case the source distribution represents the normal component of "growth" rate, and since the latter is just a function of the geometry, the source distribution can be evaluated at each section. The boundary condition equation, therefore, has the following form:

$$\sum_{k=1}^{N} A_{jk}\, \mu_k/2\pi + F_j = 0$$

where

N is the number of surface panels;

A_{jk} is the perturbation potential influence coefficient on the j^{th} control point due to unit doublet distribution on the k^{th} panel. (Note: for the panel acting on its own control point, $A_{jj} = -\pi$);

μ_k is the surface panel (k^{th}) doublet value (unknown); and

$$F_j = \phi_{\infty j} + \sum_{k=1}^{M} A_{jk}\, \mu_{wk}/2\pi + \sum_{k=1}^{N} B_{jk}\, \sigma_k/2\pi$$

where

$\phi_{\infty j}$ is the onset flow potential at the j^{th} control point;

M is the number of free-sheet panels at this time step;

μ_{wk} is the free-sheet panel (k^{th}) doublet value (known); and

B_{jk} is the perturbation potential influence coefficient on the j^{th} control point due to a unit source distribution on the k^{th} panel.

Thus, F_j can be evaluated at each time step, leaving just the μ_k values to be solved for.

At each time step, the free sheet is moved according to the local calculated velocities and a new panel is formed from the prescribed separation point, with its doublet value being related to the local vorticity value and rate of vorticity transport. Also, at each time step, the free vortex sheet is repaneled in such a way that panels are equally spaced and an appropriate vorticity distribution scheme, the details of which are presented in the next section, is evaluated.

5.0 DESCRIPTION OF BODY GROWTH AND FREE-SHEET SHEDDING MODELS

5.1 Body Growth Computational Procedure

The VORSEP pilot code is modified to incorporate the arbitrarily shaped growth of a wing geometry: the x,z coordinates, M, were read in at a preselected number of spanwise stations, N, as two-dimensional (N x M) arrays, Figure 3. This information is stored in the GEOMIN routine.

The time-stepping procedure used in the present investigation adopts the following procedure. The first calculation starts at a cross section, x_I, which is at a small distance (10% of the root chord, or so) from the apex of the wing. The initial time, (t), and the time plane, (N), are assumed to be 0 and 1, respectively. The time interval between two successive time steps is assumed to be Δt and the axial coordinate increment, $\Delta x = U_x \Delta t$, where U_x is the x-component of the onset velocity. At any time t (time plane N), $x_N = U_x t + x_I$, and the cross-sectional panel geometry is generated using the wing geometric data stored in GEOMIN.

In the previous investigation, the growth rate over the entire section under consideration is assumed to be uniform. For the arbitrarily shaped bodies considered in the present investigaton, a systematic way is devised to take into account the growth rate distribution over the entire section. At each time plane, N, the panel geometry at the next time plane, N+1, is also computed and stored and from these the growth rates and, hence, the source distributions are computed as described below.

Referring to Figure 4, the growth vector at any point, p, on a section at time plane N is given by

$$\underline{G}_p = \underline{r}_{2p} - \underline{r}_{1p} = \underline{d}_p = \underline{i} G_y + \underline{k} G_z,$$

where $Gy = y_{2p} - y_{1p}$ and $G_z = z_{2p} - z_{1p}$.

Then the source distribution at point p is given by

$$\sigma_p = (\underline{G}_p \cdot \underline{N}_p)/2\pi\Delta t$$

where $\underline{N}_p$ is the unit normal vector at point p. Thus at the time plane, N, from the known (stored) panel geometries at two consecutive cross sections (time planes N and N+1), the growth rate distribution and, hence, the source distribution needed in the aerodynamic calculation at each panel center point is computed.

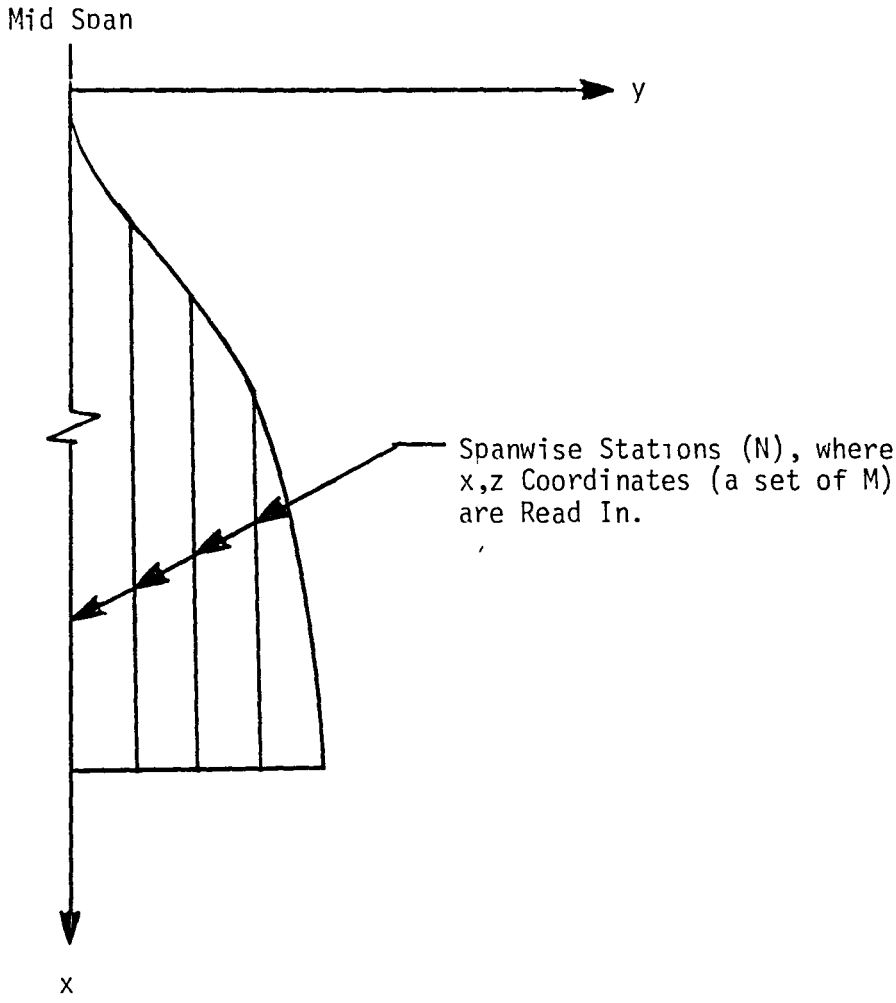

Figure 3. Geometry Definition of a Wing.

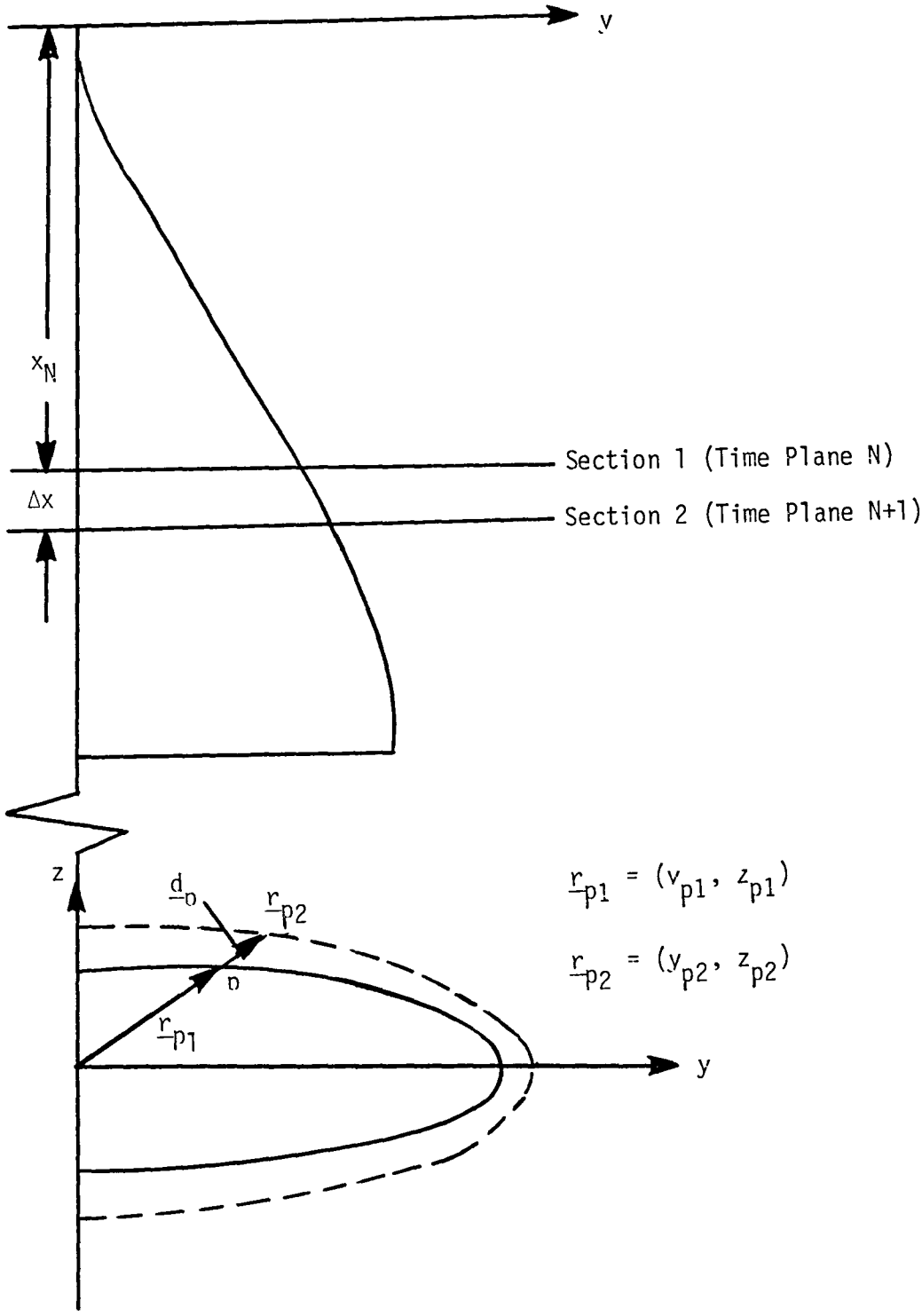

Figure 4. Model for Computation of Growth Rate Distribution over a Cross Section.

5.2 Free-Sheet Shedding and Redistribution Model

The free-sheet routine in VORSEP introduces an additional panel and a point vortex (at the end of the panel) at each time step. While this simple technique yielded acceptable solutions for a thin flat plate and a thick elliptic section with carefully selected Δt's and merge angles for vortex roll-up, it is not able to handle the complex flow field associated with the separation near a sharp thick edge. The new free-sheet shedding and vorticity distribution model is described below.

Figure 5 illustrates the free-sheet shedding model. The doublet values are associated with the panel corners rather than the panel centers and they remain constant with time. At each new time step, the doublet value at the separation (corner point) is computed by interpolating the doublet (μ) and the vorticity (γ) values on the upper and lower surfaces separately. The width of the first wake panel, $s_1 = \Delta t\ V_{sep}$, where V_{sep} is the velocity at the separation point. The doublet values at the beginning (separation point) and the end of the first free-sheet panel are given by

$$\mu_{sep} = (\mu_u - \mu_\ell) + s_1(\gamma_u + \gamma_\ell)$$

and

$$\mu_1 = \mu_u - \mu_\ell.$$

The doublet values at the other free-sheet corner points take the preceding values such as $\mu_2 = \mu_{1p}$ (previous value at the end of the first free-sheet panel), etc.

Additionally, the free-sheet panels and the doublet values are redistributed after each time step in such a way that they are uniformly spaced along the free sheet. This scheme allows us to increase or decrease the number of free-sheet panels, thereby providing the flexibility to adjust the free-sheet panel sizes to be compatible with the surface panels regardless of the time step size. The amalgamation procedure in VORSEP is kept (see (7)).

This new free-sheet model combined with the redistribution scheme has proven very successful. The free-sheet vortex roll-up for several θ_{merge} values on an 8.5% thick triangular-shaped cross section with a flat upper surface and with a prescribed separation location is presented in Figure 6. This figure demonstrates the success of the present redistribution scheme in alleviating the problem of numerical instabilities associated with the uneven distribution of wake panels. Good numerical stability is absolutely essential if the calculations are to reach the large times representing the traverse over a complete wing chord.

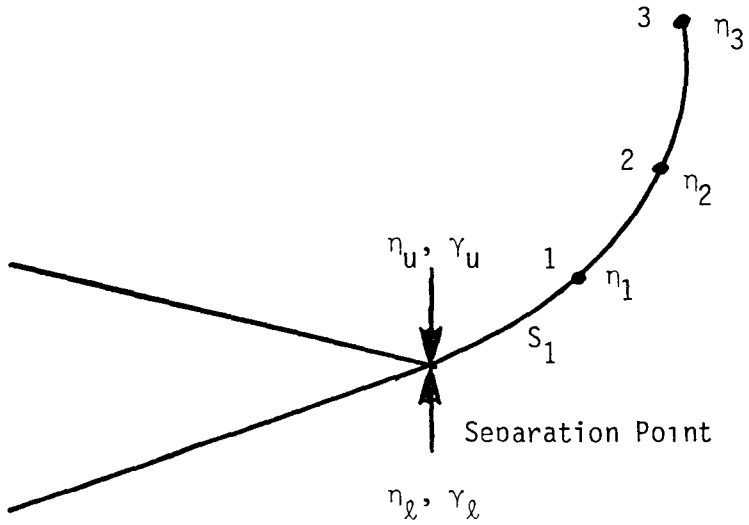

1, 2, 3, etc. - Panel Corner Points

$\eta_1 = \eta_u - \eta_\ell$

$\eta_{sep} = \eta_1 + S_1(\gamma_u + \gamma_\ell)$

Figure 5. Free-Sheet Shedding Model.

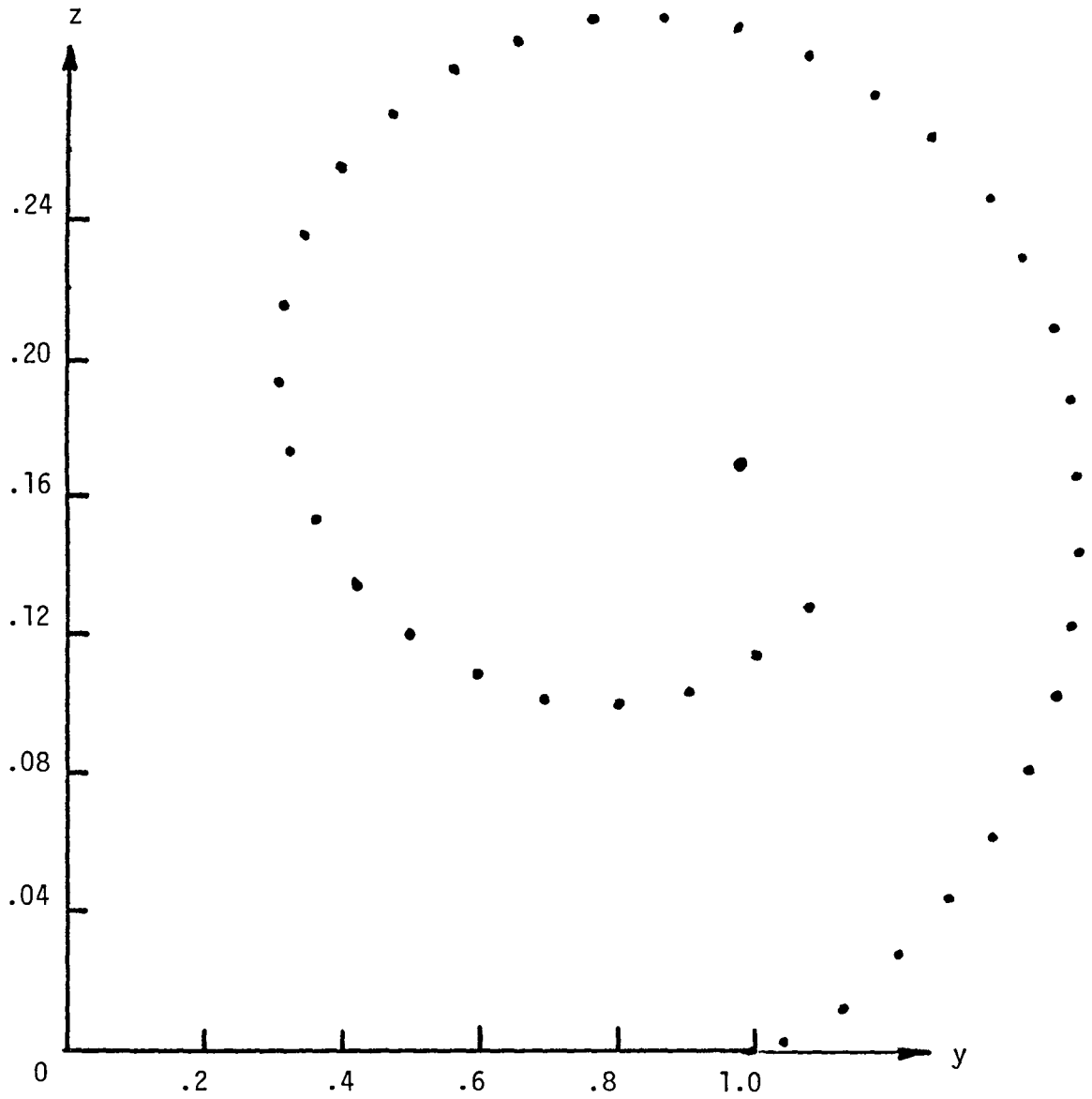

Figure 6. The Vortex Structure.

(a) $\theta_{merge} = 400°$.

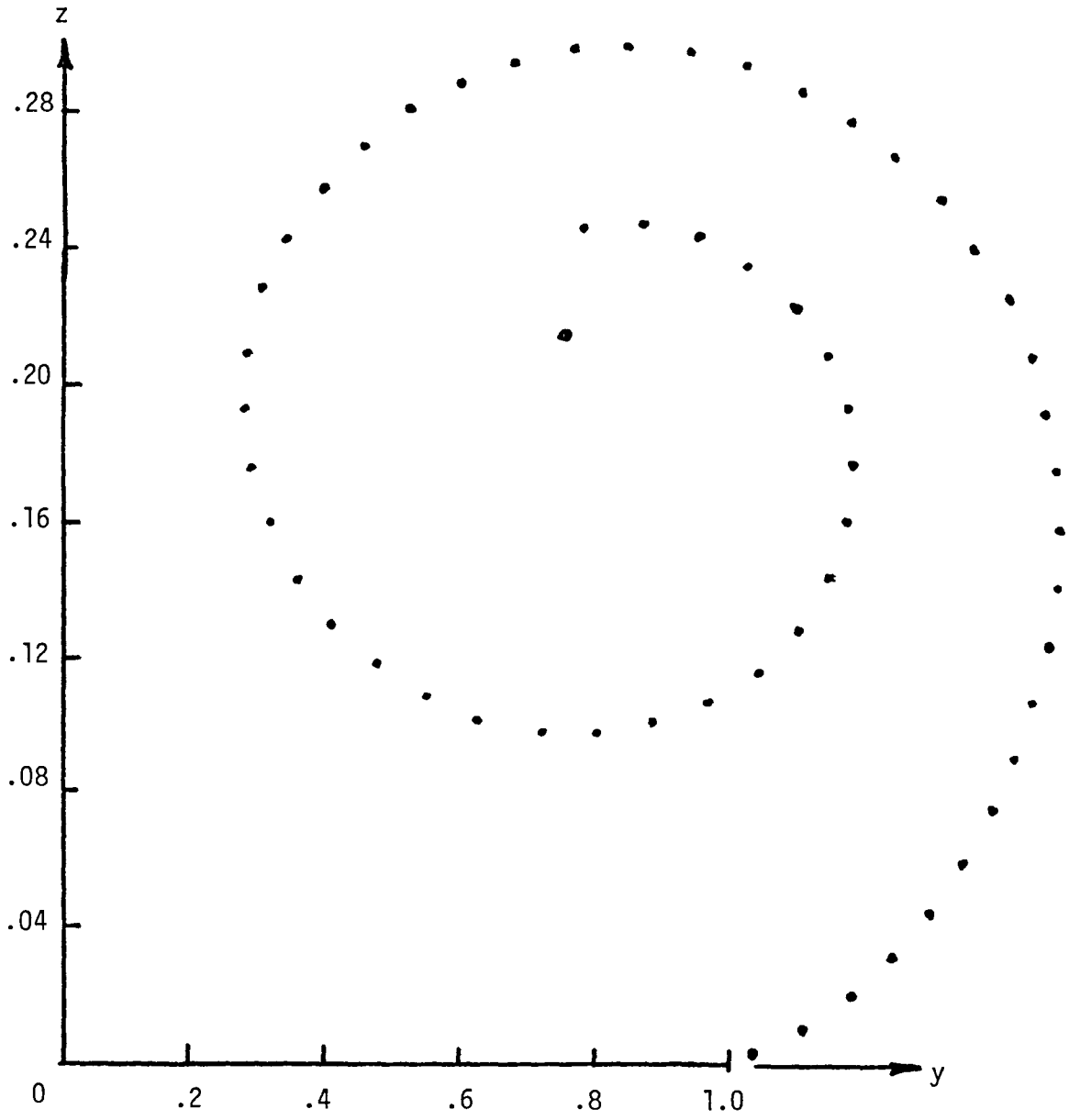

Figure 6. Continued.

(b) $\theta_{merge} = 540°$.

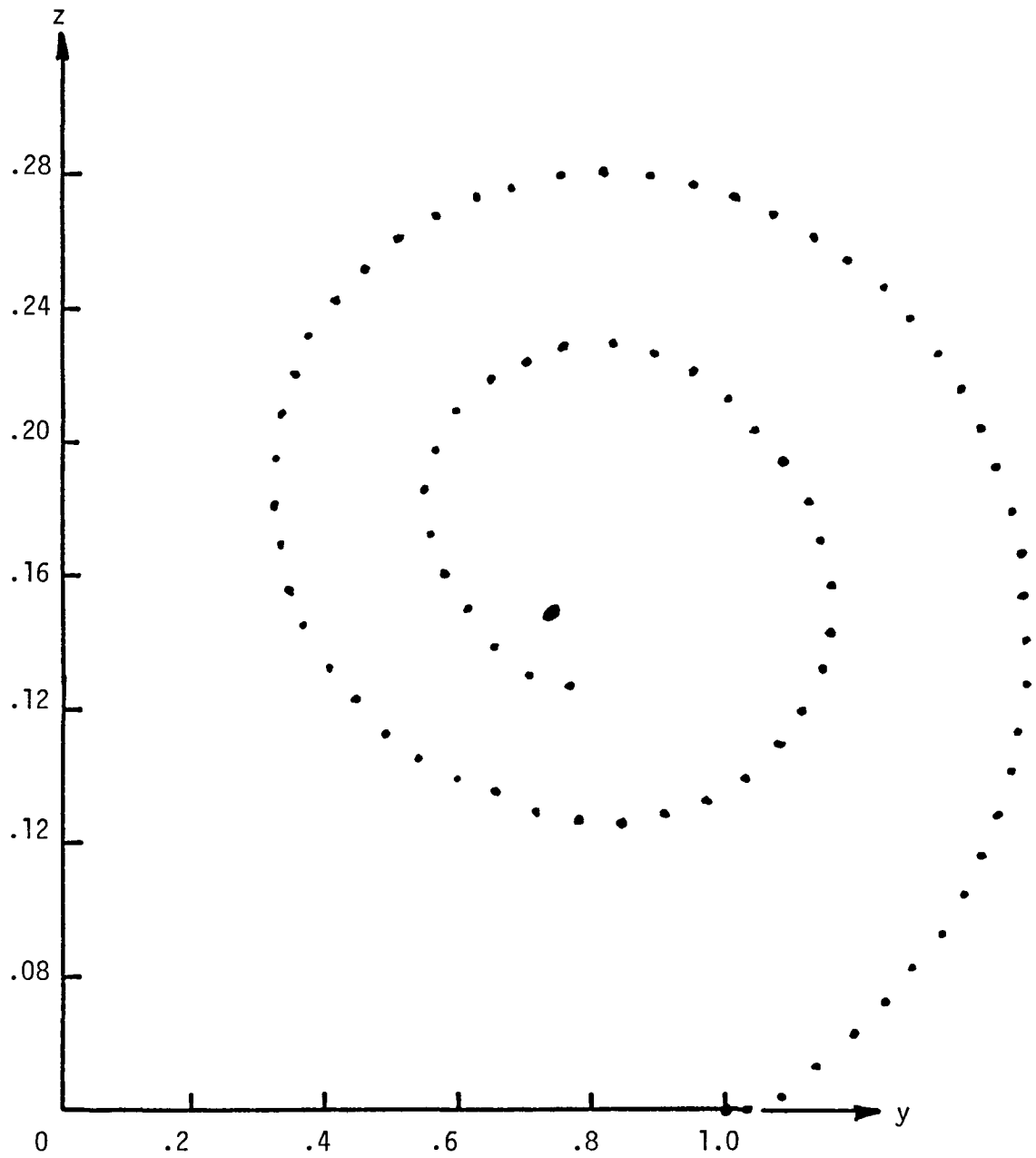

Figure 6. Concluded.

(c) $\theta_{merge} = 720°$.

6.0 DISCUSSION OF RESULTS

The three-dimensional wing geometry is reduced to a set of cross-flow plane sections for the unsteady two-dimensional analysis. The relationship between successive section shapes determines the growth rate which is represented by a source distribution in the two-dimensional calculation. The onset flow at each cross-flow station is the vertical component of the general onset flow.

This model is incorporated in the VORSEP code along with a refined free-sheet shedding and redistribution model as discussed in the previous section. The code is applied to several test cases.

6.1 Thin Triangular Delta Wing (10)

Figure 7 shows the shape of the vortex free sheet at several cross sections. The calculation started at $x/c = 0.1$ ($t = 0$). The computed vortex core positions and the experimental suction peaks are compared in Figure 8 and they are in good agreement. The fluctuation in the computed vortex core position is due to the merging procedure and the finite vorticity carried in the vortex sheet. Note that the actual vortex centroid may be slightly different from the vortex core location due to the merging process.

The calculation used a θ_{merge} angle of 180° which approximates current practice in the Boeing LEV code. However, calculations have been performed with θ_{merge} values as high as 720° with stable solutions (see Figure 6); the closer detail this gives for the first passage of the free sheet near the surface offers better definition of the surface pressure distribution than is given by the earlier amalgamation.

6.2 Ogee Wing (11)

A series of vortex sheet shapes is shown in Figure 9 from the calculated set for 21° angle of attack. The calculation started at $x/c_R = .1$, and a total of 90 time planes were calculated. It is interesting to observe the changes in the initial shape of the sheet as it leaves the surface at various stations; i.e., the influence of the leading-edge sweep of rate of growth in the two-dimensional calculation. Also, the ellipticity in the shape of the sheet is very pronounced in the region of smallest sweep (maximum growth rate). The amalgamation angle was set at 360° for these calculations in order to represent the first passage of the free sheet over the surface.

A planform view is given in Figure 10, which compares the amalgamation point (not the vorticity centroid) with the surface flow features from experiment. The path is somewhat outside the experimental location, but this is probably because we are not representing the secondary vortex. In principle, we could release a secondary vortex from a prescribed location at any of the time steps.

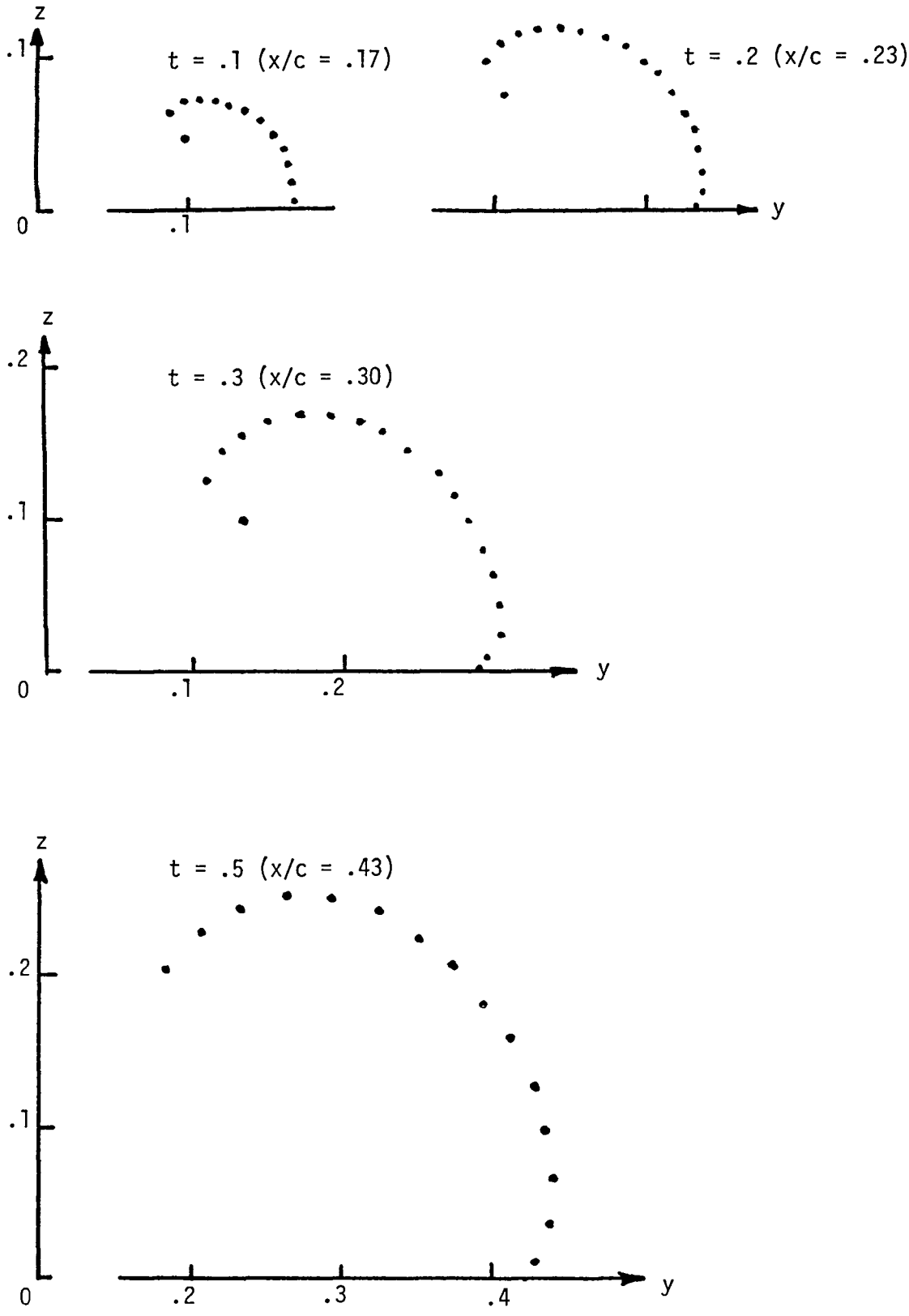

Figure 7. History of the Vortex Structure on the Growing Thin Delta Wing. Semispan (b/2) = 1; AR = 1; Leading-Edge Sweep Angle = 75.96°; α = 20.5°; θ_{merge} = 180°.

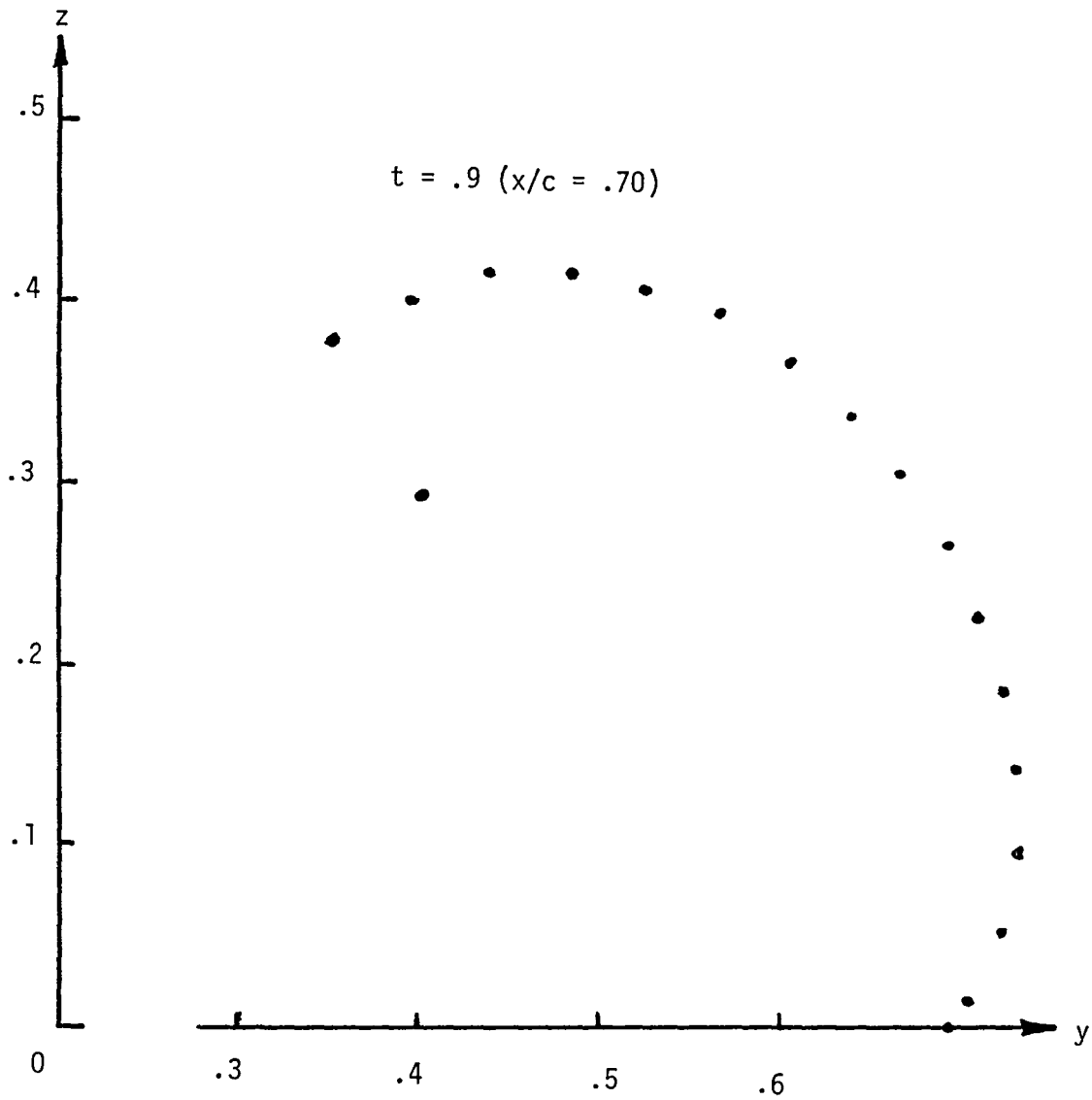

Figure 7. Continued.

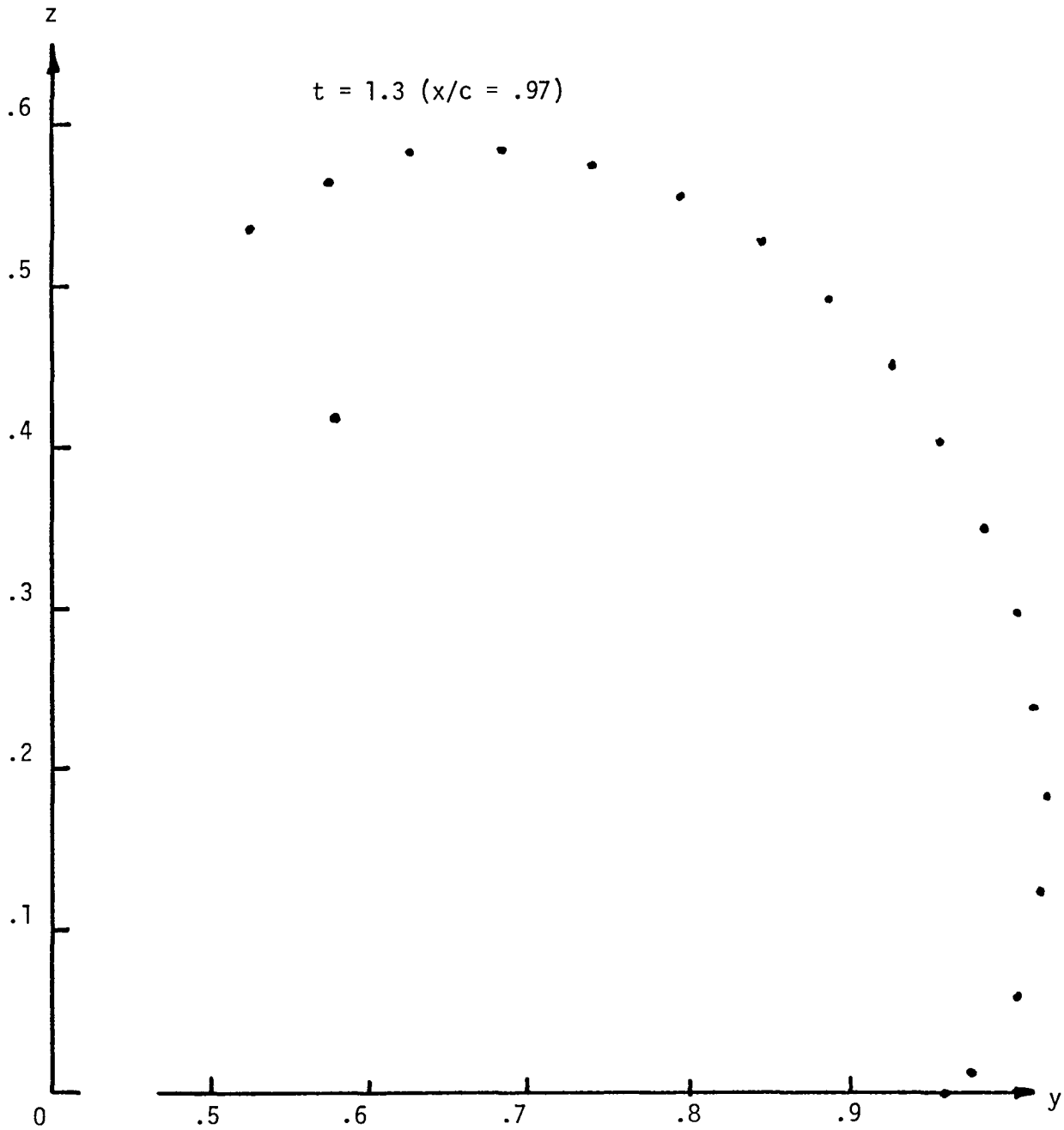

Figure 7. Concluded.

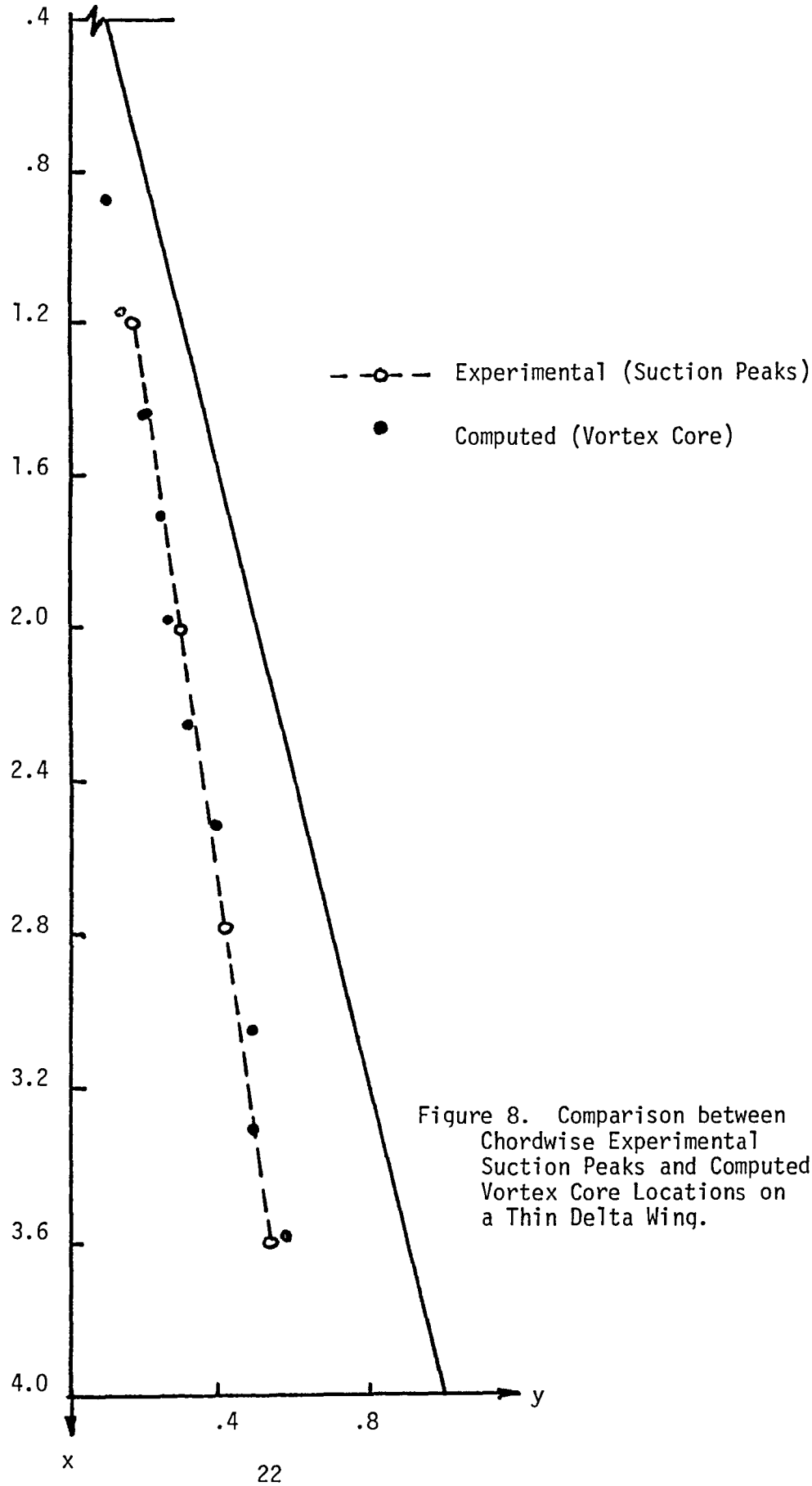

Figure 8. Comparison between Chordwise Experimental Suction Peaks and Computed Vortex Core Locations on a Thin Delta Wing.

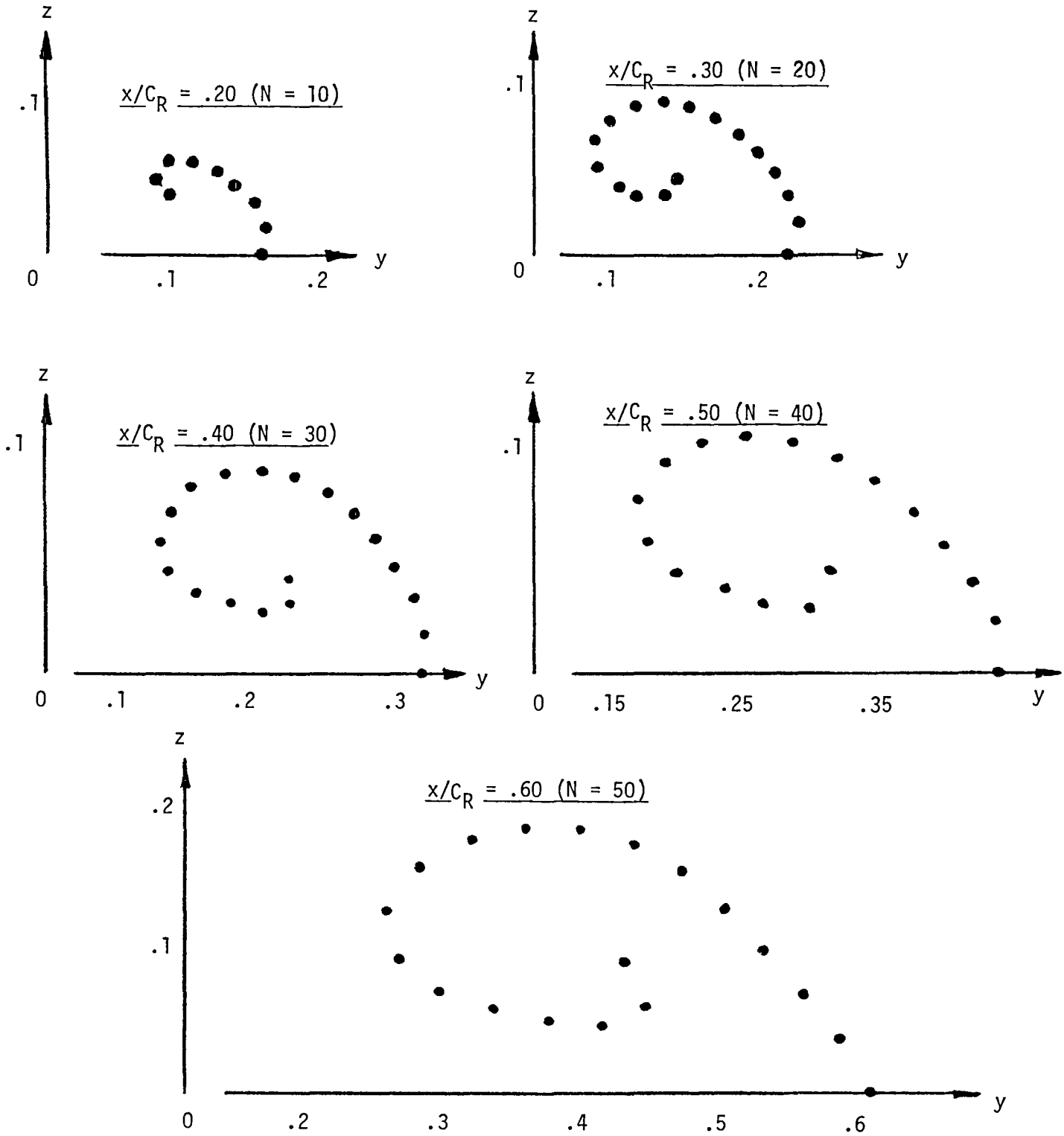

Figure 9. Ogee Wing (α = 21°).

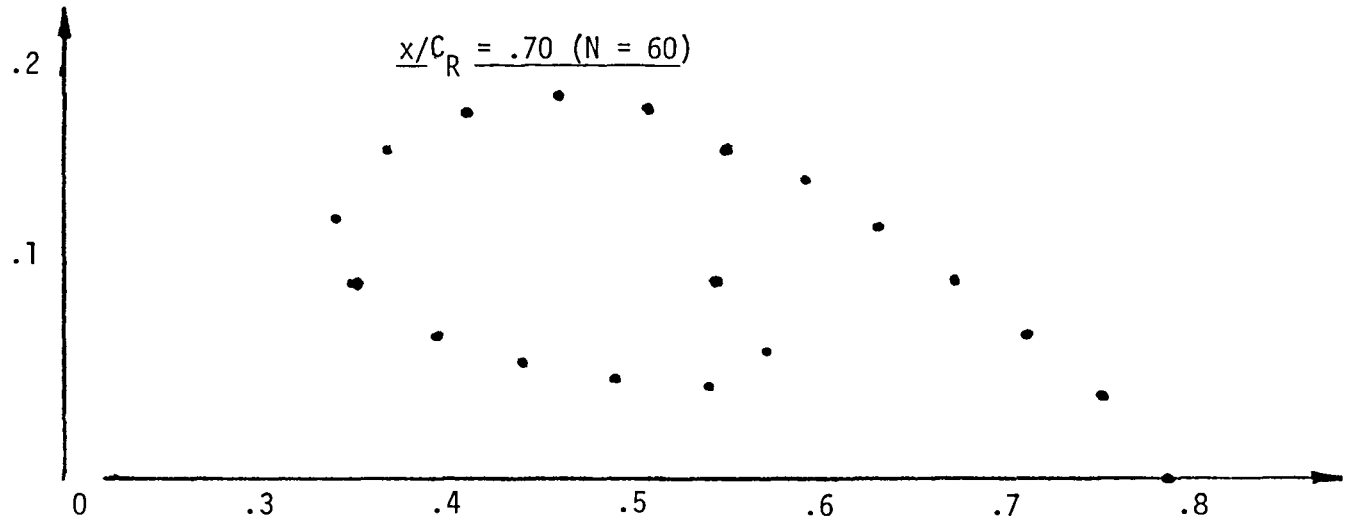

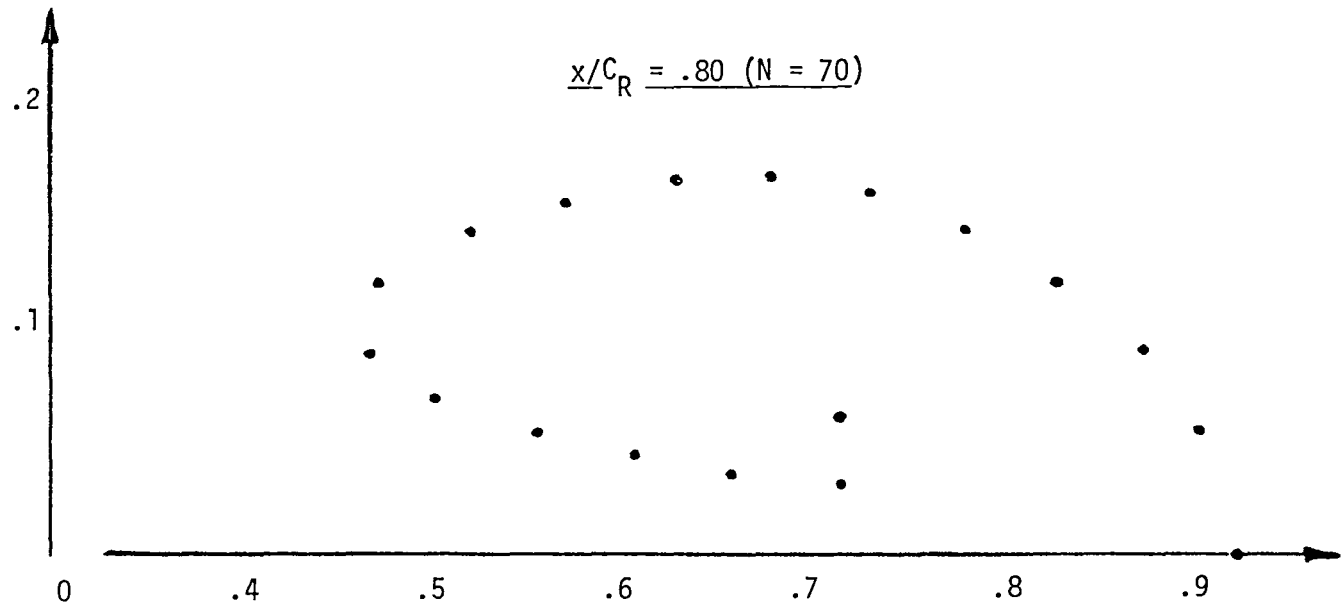

Figure 9. Concluded.

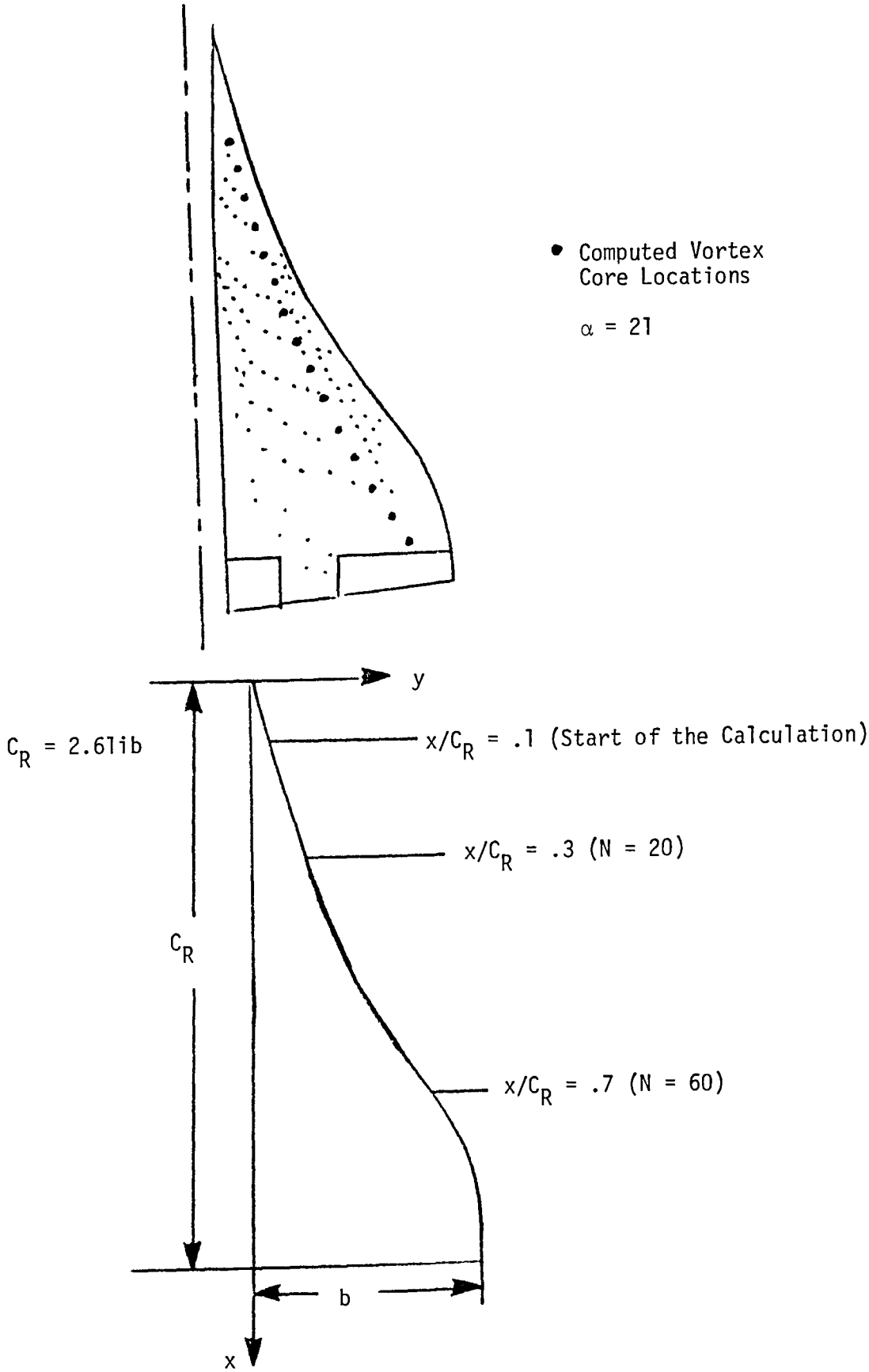

Figure 10. Computation Model for Ogee Wing.

6.3 Bent Rectangular Wing (12)

A rectangular wing of aspect ratio 1/4 and with a 20° mid-chord bend has been tested in order to demonstrate a strong camber effect. The model is set at 20° incidence giving a 40° angle of attack to the flow on the rear portion. The experimental observations clearly show a double vortex system--one from the leading edge, the other from the kink. The calculation started at $x/c = 0.1$ and a total of 81 time planes were calculated. Vortex structures are shown in Figure 11 at a number of stations downstream of the kink. Although a definite bulge has appeared in the free sheet, the detailed roll-up of the second vortex has been smeared out by our redistribution scheme. A higher density of wake panels would improve the definition of the bulge and, hence, the local roll-up. Even so, the bulge does migrate around the main vortex (Figure 11(c) through (g)) in a similar way to the experimentally observed second vortex (see Figure 5, Ref. 12). An intermediate amalgamation scheme covering the second vortex would improve the numerical behavior of the calculation.

The calculated doublet distribution along the free sheet is shown in Figure 12. Distance s is measured along the sheet from the separation point. The gradient of the doublet distribution (i.e., the vorticity value) takes a sudden increase at the point corresponding to the piece of free sheet shed from the bend in the plate. The kink in the doublet distribution corresponds to the location of the second vortex as it migrates along the free sheet. Figure 12(b) shows the condition at a later time plane: the distortion in the doublet distribution near the kink is caused by the secondary roll-up. This secondary roll-up is clearly being transported along the free sheet and will eventually be amalgamated in the main core. Although the results are preliminary, they look promising for this extreme case.

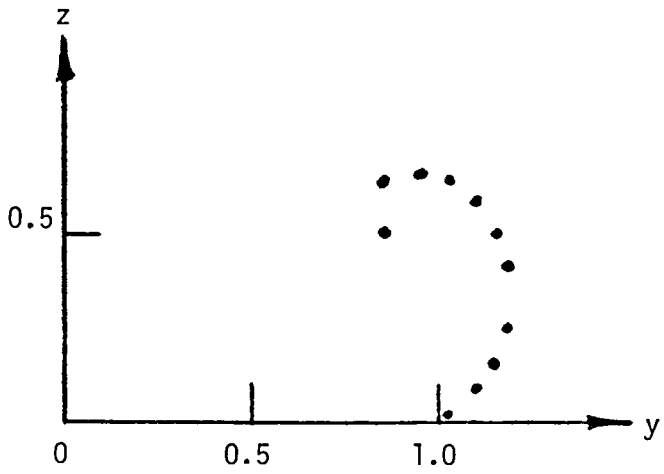

(a) x/c = 0.377; N = 20.

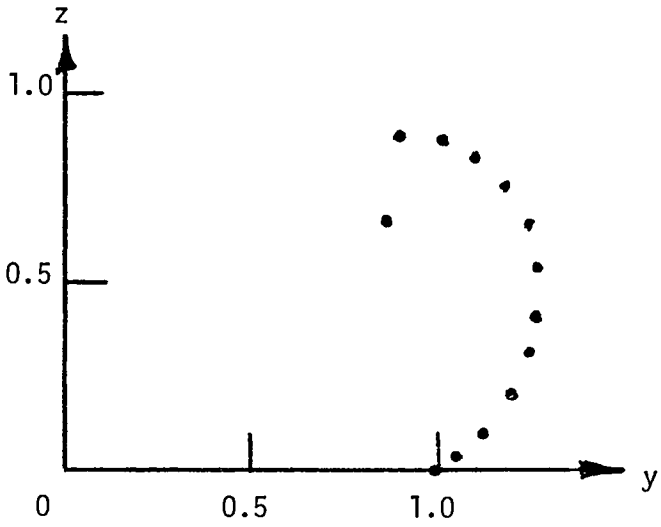

(b) x/c = 0.461; N = 40.

Figure 11. Bent Plate (α = 20°).

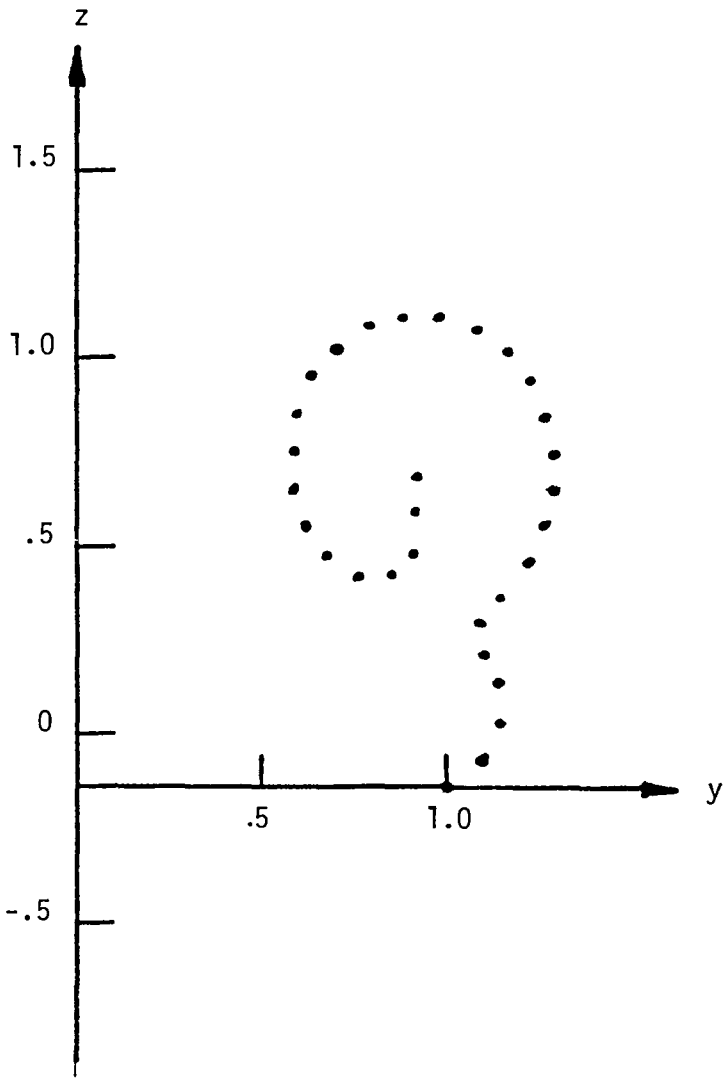

Figure 11. Continued.

(c) x/c = 0.544; N = 40.

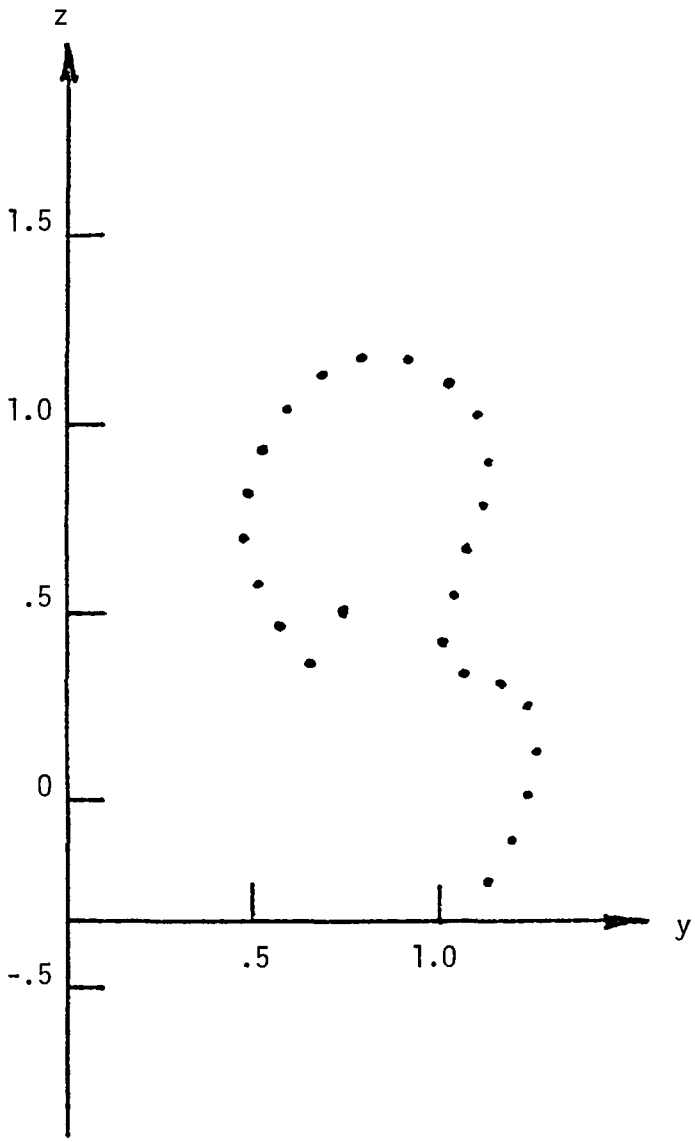

Figure 11. Continued.

(d) x/c = 0.60; N = 45.

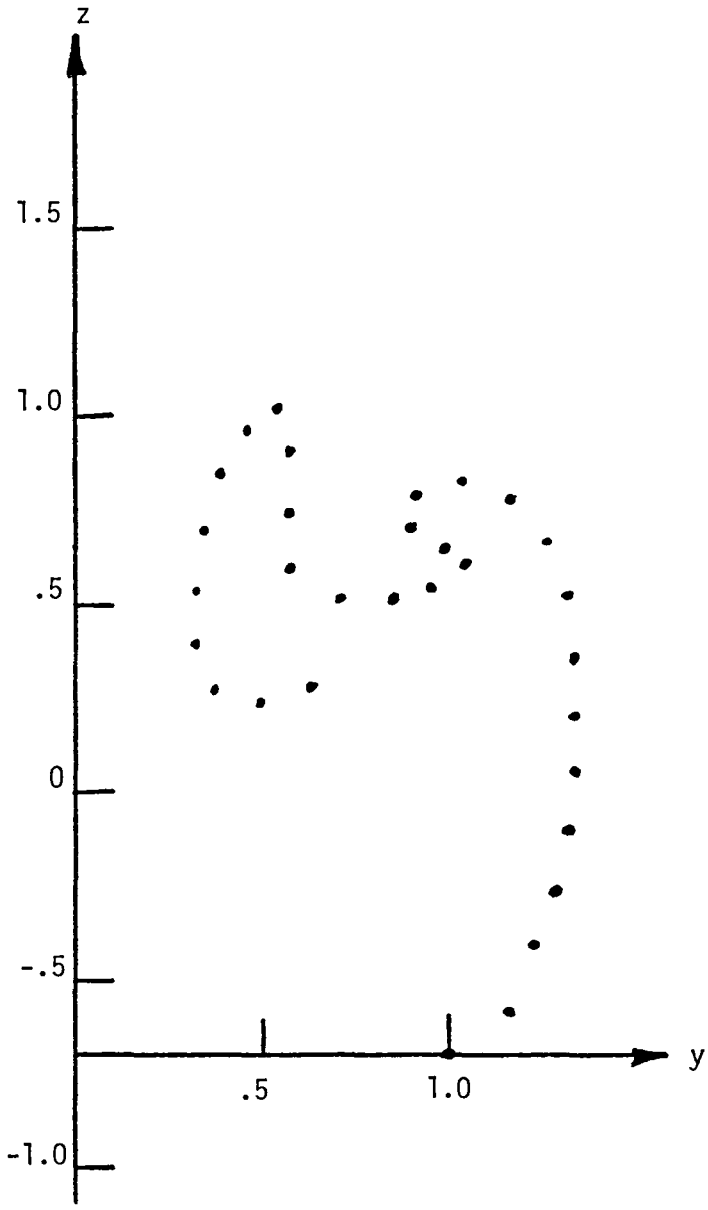

Figure 11. Continued.

(e) x/c = 0.711; N = 55.

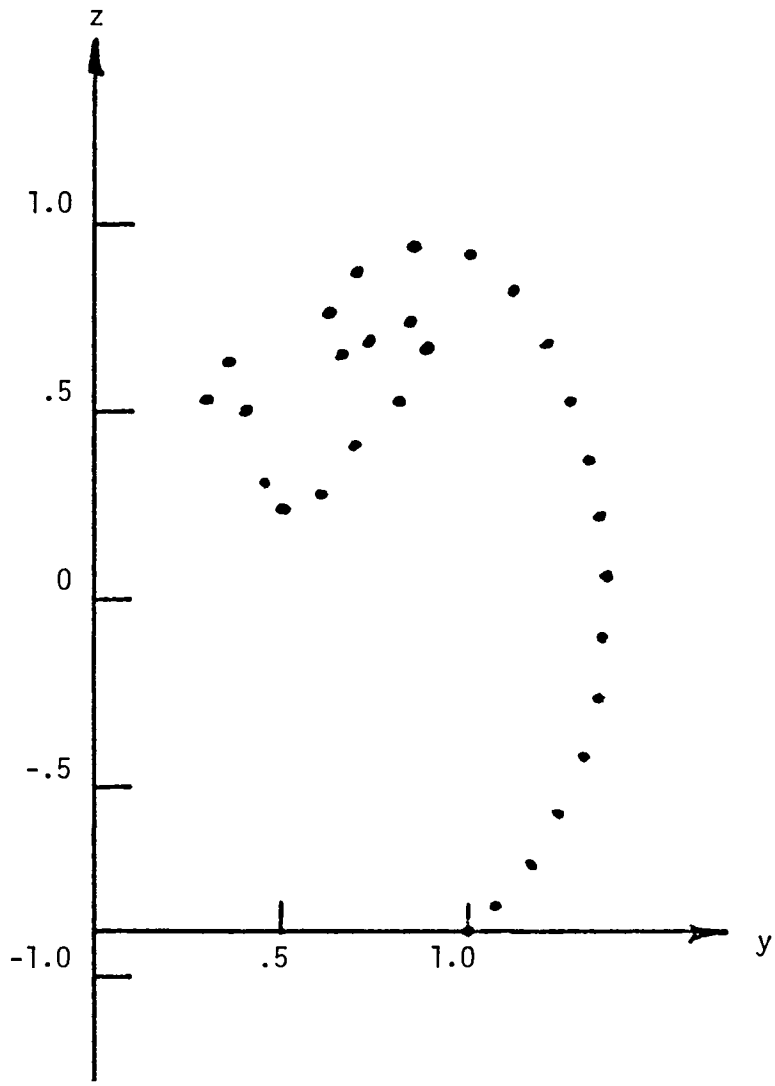

Figure 11. Continued.

(f) x/c = 0.767; N = 60.

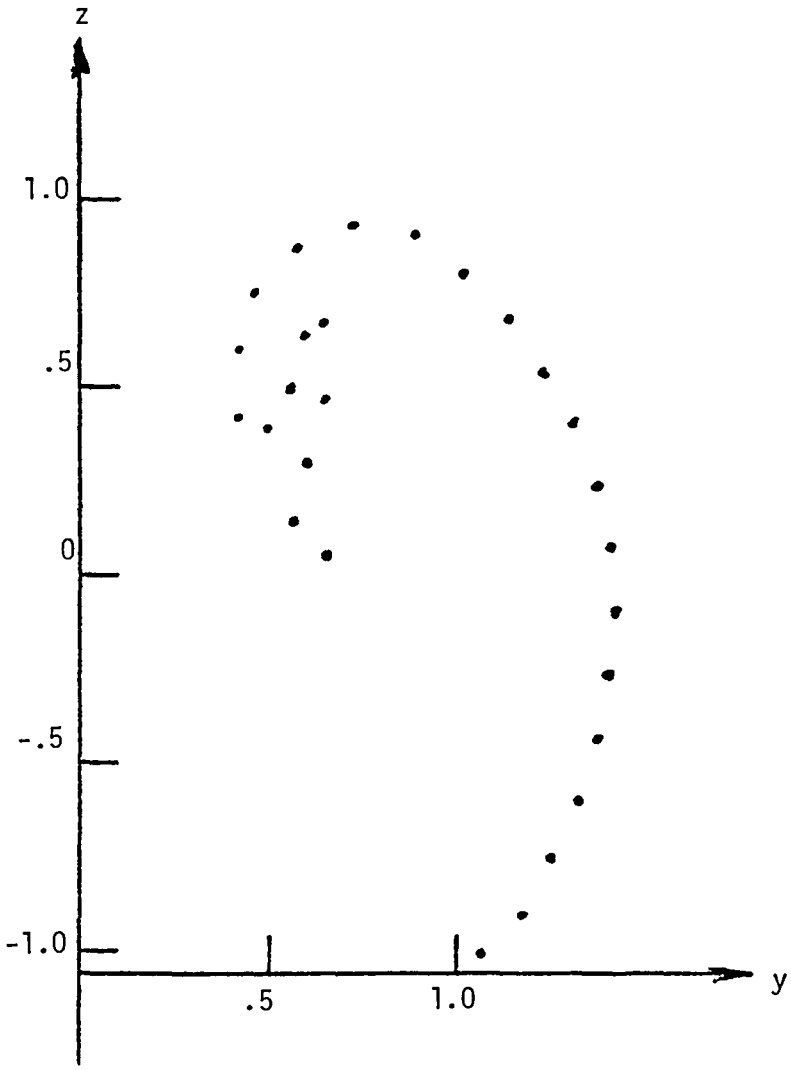

Figure 11. Concluded.

(g) x/c = 0.822; N = 65.

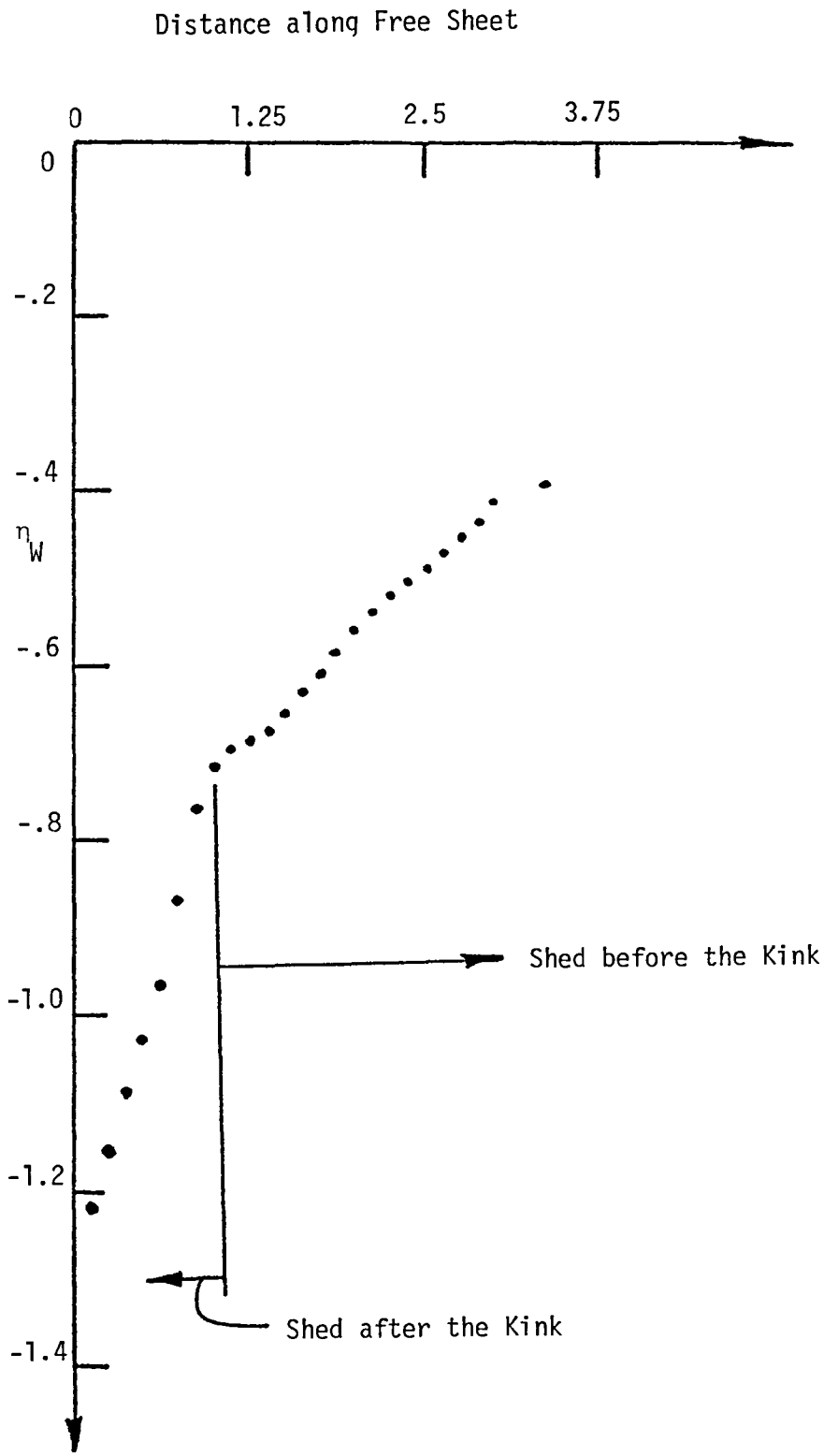

Figure 12. Calculated Doublet Distribution along the Free Sheet.

(a) x/c = 0.60; N = 45.

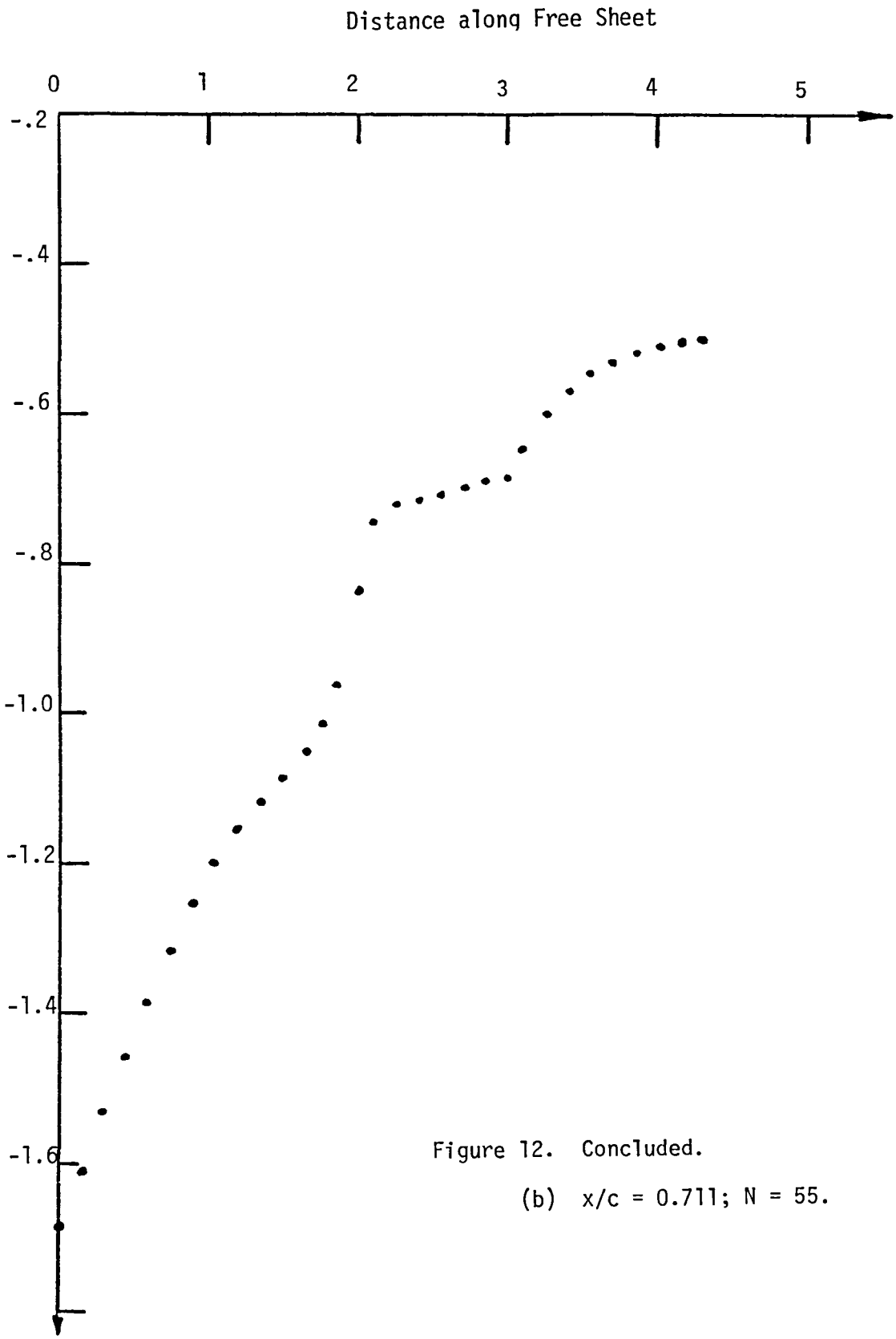

Figure 12. Concluded.

(b) x/c = 0.711; N = 55.

7.0 CONCLUSIONS

An improved wake shedding model combined with a doublet distribution scheme along the free sheet alleviated the numerical instabilities associated with the free vortex sheet. Using this improved scheme, calculations have been performed with θ_{merge} values as high as 720° with a stable and well defined rolled up vortex.

An automatic procedure to define the geometry and the source distribution over each cross section as a function of time is incorporated into the VORSEP program. The modified program is validated by successfully applying it to a few test cases.

8.0 RECOMMENDATIONS FOR FURTHER WORK

In the present investigation, the calculations started at 1/10 of the semispan (see Figure 13); this means that this station is the commencement of separation in the calculation. The growing body calculation must start with an actual shape. It is recommended that in future work the starting conditions will include the conical flow solution over the forward part of the planform, Figure 13.

Currently, the calculations cease at the trailing edge, and this must be unswept. Extensions of the coding are recommended which will allow the body to disappear from the calculation plane; i.e., leaving just the free sheet and the vortex core together with the trailing sheet from the trailing edge. It is further proposed to extend this capability by allowing the body to disappear gradually from the calculation plane. This would allow both positive and negative sweepback on the trailing edge, Figure 14.

The preprocessor code is currently an independent code. It is recommended to develop interfacing routines with the Boeing LEV code so that the existing use definition of the LEV code is disturbed as little as possible.

Finally, the coupled code should be exercised over a range of conditions. The investigation should include convergence studies on pressures, forces and vortex location.

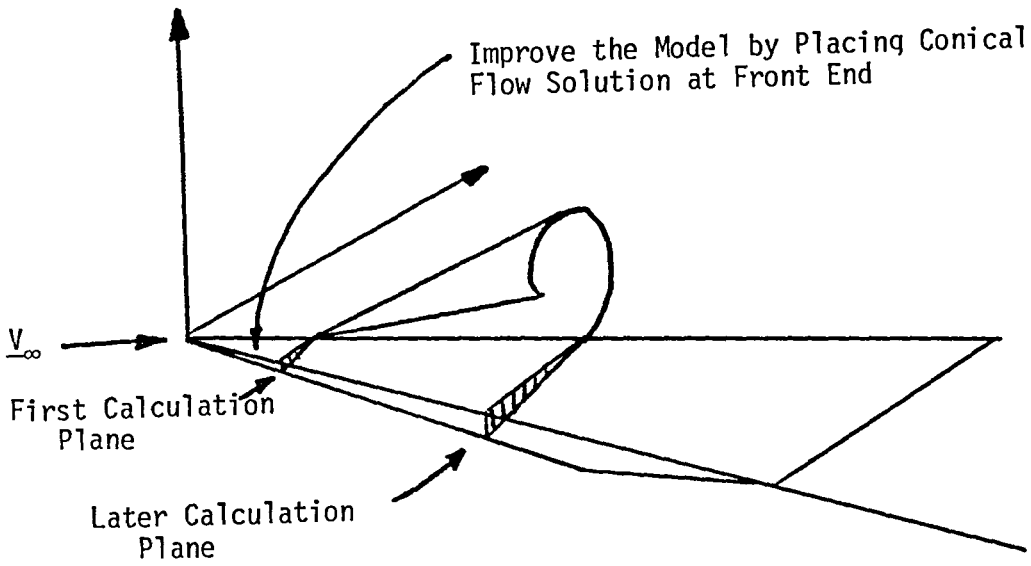

Figure 13. Recommended Change to the Flow Model.

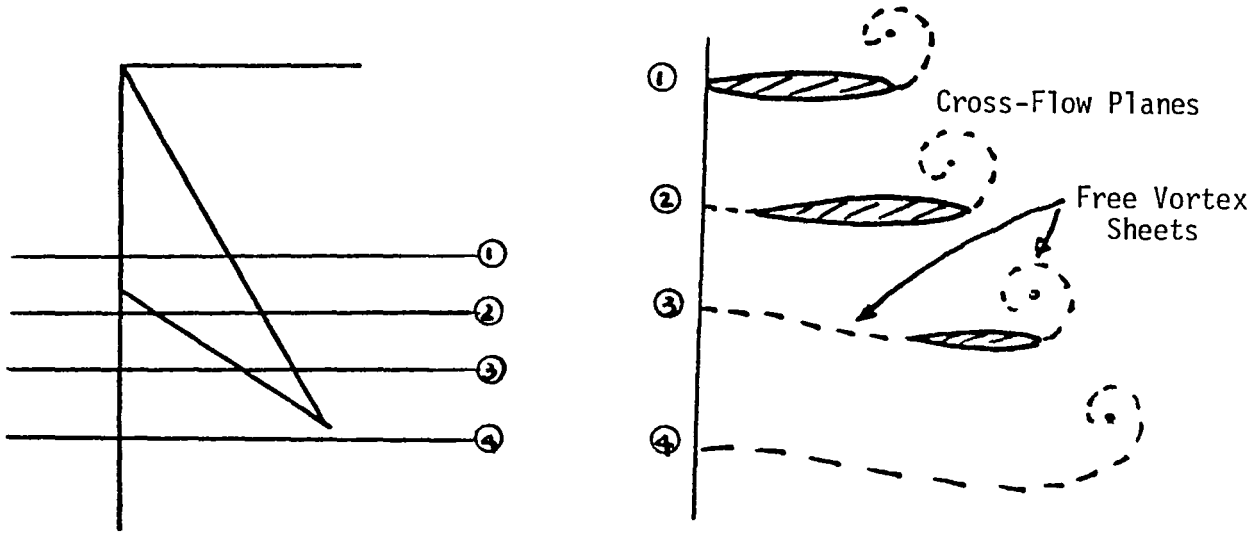

Figure 14. Recommended Extension of Method Scope.

9.0 REFERENCES

1. Smith, J.H.B., "Inviscid Fluid Models Based on Rolled Up Vortex Sheets for Three-Dimensional Separation at High Reynolds Number", Paper No. 9, AGARD Lecture Series No. 94 on Three-Dimensional and Unsteady Separation at High Reynolds Numbers, February 1978.

2. Polhamus, E.C., "Predictions of Vortex Lift Characteristics by a Leading-Edge Suction Analogy", J. Aircraft, Vol. 8, 1971, p. 193.

3. Brown, C.E. and Michael, W.H., "On Slender Delta Wings with Leading-Edge Separation", NACA TN-3430, 1955.

4. Mangler, K.W. and Smith, J.H.B., "A Theory of Flow Past a Slender Delta Wing with Leading-Edge Separation", Proceedings Royal Society, London, Ser. A, 251, 1959, p. 200.

5. Smith, J.H.B., "Improved Calculations of Leading-Edge Separation from Slender, Thin Delta Wings", Proceedings Royal Society, London, Ser. A, 306, 1968, pp. 67-90.

6. Johnson, F.T. et al., "An Improved Panel Method for the Solution of Three-Dimensional Leading-Edge Vortex Flows", Vol. I--Theory Document, NASA CR-3278; Vol. II--User's Guide and Programmer's Document, NASA CR-3279, 1980.

7. Maskew, B., "Calculation of Two-Dimensional Vortex-Surface Interference Using Panel Methods", NASA CR-159334, December 1980.

8. Maskew, B., "Program VORSEP, Interim Pilot Code, Method Description and User Guide", NASA Contract NAS1-15495, Analytical Methods, Inc., December 1979.

9. Marshall, F.J. and Deffenbaugh, F.D., "Separated Flow over a Body of Revolution", J. Aircraft, Vol. 12, No. 2, pp. 78-85, February 1975.

10. Hummel, D., "On the Vortex Formation over a Slender Wing at Large Angles of Incidence", High Angle of Attack, U.S. Department of Commerce, NTIS AD-A067323, January 1979.

11. Collard, D., "Comportement a Haute Incidence D'un Avion de Transport a Aile a Grand Elancement", U.S. Department of Commerce, NTIS, AD-A067323, January 1979.

12. Wickens, R.H., "The Vortex Wake and Aerodynamic Load Distribution of Slender Rectangular Wings", Canadian Aeronautics and Space Journal, June 1967, pp. 247-260.

1 Report No	2 Government Accession No	3 Recipient's Catalog No
NASA CR-165858		

4 Title and Subtitle	5 Report Date
FLOWS OVER WINGS WITH LEADING-EDGE VORTEX SEPARATION	April 1982
	6 Performing Organization Code
7 Author(s)	8 Performing Organization Report No
B.M. Rao and B. Maskew	8105
	10 Work Unit No
9 Performing Organization Name and Address	11 Contract or Grant No
Analytical Methods, Inc. 2047 - 152nd Avenue N.E. Redmond, Washington 98052	NAS1-16155
	13 Type of Report and Period Covered
12 Sponsoring Agency Name and Address	Contractor Report
NASA Langley Research Center Hampton, Virginia 23665	14 Sponsoring Agency Code

15 Supplementary Notes

16 Abstract

A doublet code (VORSEP) is extended to reduce the three-dimensional steady flow problem of arbitrarily shaped swept wings with leading-edge separation into an unsteady two-dimensional flow problem in which the section shape changes with time. The time-stepping procedure and the code are successfully tested by application to several test cases.

17 Key Words (Suggested by Author(s))	18 Distribution Statement
Vortex Flow Vortex Separation Unsteady Flow Leading-Edge Separation Vortex Roll-up	Unclassified - Unlimited

19 Security Classif (of this report)	20 Security Classif (of this page)	21 No of Pages	22 Price
Unclassified	Unclassified	39	

N-305

For sale by the National Technical Information Service, Springfield, Virginia 22161

NASA Contract Report 165858

DISTRIBUTION LIST

NAS1-16155

	No. of Copies
NASA Langley Research Center Hampton, VA 23665	
Attn: Report and Manuscript Control Office, Mail Stop 180A	1
Technical Utilization Office, Mail Stop 139A	1
W. E. Schoonover, Mail Stop 294	24
NASA Ames Research Center Moffett Field, CA 94035	
Attn: Library, Mail Stop 202-3	1
NASA Dryden Flight Research Center P. O. Box 273 Edwards, CA 93523	
Attn: Library	1
NASA Goddard Space Flight Center Greenbelt, MD 20711	
Attn: Library	1
NASA Lyndon B. Johnson Space Center 2101 Webster Seabrook Road Houston, TX 77058	
Attn: JM6/Library	1
NASA Marshall Space Flight Center Marshall Space Flight Center, AL 35812	
Attn: Library, AS24L	1
Jet Propulsion Laboratory 4800 Oak Grove Drive Pasadena, CA 91103	
Attn: Library, Mail Code 111-113	1
NASA Lewis Research Center 21000 Brookpark Road Cleveland, OH 44135	
Attn: Library, Mail Stop 60-3	1
NASA John F. Kennedy Space Center Kennedy Space Center, FL 32899	
Attn: Library, NWSI-D	1
National Aeronautics and Space Administration Washington, DC 20546	
Attn: RTF-6	1
NASA Scientific & Technical Information Facility 6571 Elkridge Landing Road Linthicum Heights, MD 21090	30 plus original

End of Document